Dynamic Control of Cardiac Alternans

Kevin Hall,[1] David J. Christini,[2] Maurice Tremblay,[3] James J. Collins,[2] Leon Glass,[1] and Jacques Billette[3]

[1]*Departments of Physics and Physiology, McGill University, Montreal, Quebec, Canada*
[2]*Neuromuscular Research Center and Department of Biomedical Engineering, Boston University, Boston, Massachusetts*
[3]*Départment de Physiologie, Faculté de Médecine, Université de Montréal, Montreal, Quebec, Canada*

A dynamic control technique was used to suppress a cardiac arrhythmia called an alternans rhythm in a piece of dissected rabbit heart. Our control algorithm adapted to drifting system parameters, making it well suited for the control of physiological rhythms. Control of cardiac alternans rhythms may have important clinical implications since they often precede serious cardiac arrhythmias and are a harbinger of sudden cardiac death. [S0031-9007(97)03337-1]

Control techniques from the field of nonlinear dynamics [1] have been used to control both chaotic [2] and nonchaotic [3] dynamical systems. Since these control methods do not require knowledge of the system's governing equations, they are particularly applicable in biology where detailed mathematical models are usually unavailable. Control of biological dynamics is important for medical science since abnormal physiological rhythms can be life threatening [4]. Attempts have already been made to control both experimental [5] and model [6,7] biological systems. However, none of these studies used control algorithms which adapted to evolving system parameters. Since physiological environments typically drift over time, practical biological control schemes must adapt to these changes. Here, we utilize an algorithm which controls an evolving cardiac arrhythmia called an alternans rhythm in the rabbit heart.

Cardiac alternans rhythms are characterized by an alternation of the timing or morphology of the heart's electrical activity from one beat to the next. While the clinical importance of cardiac alternans has only recently been recognized [8], their discovery dates back to the earliest recordings of cardiac electrical signals [9]. We generated cardiac alternans by electrically stimulating a piece of dissected rabbit heart [10]. Each stimulus delivered to the upper atrium caused a wave of electrical activity to propagate through the atrium, the atrioventricular (AV) node and out the His bundle which is the output of the AV node [Fig. 1(a)]. We measured the electrical activity near an atrial input of the AV node and at the His bundle output [Fig. 1(b)]. X was the time for the impulse to pass through the AV node. The output impulse was reinjected into the atrium after a time delay λ. When λ was made sufficiently small, the conduction time through the AV node began to alternate [11] [Fig. 1(b)].

The dynamics of AV nodal conduction can be characterized by a one-dimensional map

$$X_{n+1} = f(X_n, \lambda), \tag{1}$$

where X_n is the AV nodal conduction time following the nth atrial stimulus, λ is the time delay from His bundle

activation to the next atrial stimulus, and f is a nonlinear, decreasing function of both arguments which relates the successive conduction times [11]. The map is represented as a graph in Fig. 2(a). This map determines the sequence of AV nodal conduction times, $X_1, X_2, X_3, \ldots, X_n$ given some initial conduction time, X_0, for fixed λ. The intersection of the curve with the line of identity ($X_{n+1} = X_n$) defines the period-1 fixed point $X^* = f(X^*, \lambda)$. If $|\frac{\partial f}{\partial X}| < 1$ at X^*, then X^* is stable and the sequence of conduction times will converge to X^* [Fig. 2(a)]. If $\frac{\partial f}{\partial X}$ at X^* becomes less than -1, then X^* loses stability and a period-2 cycle gains stability. In our preparation, this period-doubling bifurcation causes the alternans rhythm [11]. For example, Fig. 2(b) shows a sequence of conduction times diverging from the fixed point (dashed arrows) and the development
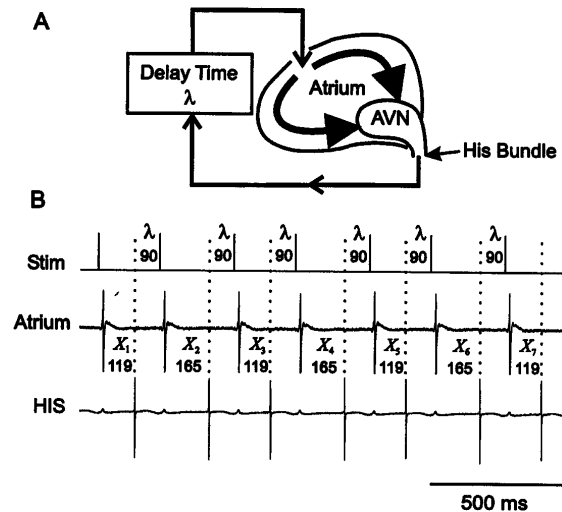
FIG. 1. (a) Schematic diagram of the rabbit heart preparation and pacing strategy. Following detection of His bundle (HIS) activation, we applied the next atrial stimulus after a time delay, λ, which was our control parameter. (b) Stimulation pulses and electrograms recorded from the atrium and His bundle during alternans. The conduction time, X, through the atrioventricular node (AVN) was defined as the time interval between atrial and His bundle deflections. Here we show an alternation of X between 119 and 165 ms for $\lambda = 90$ ms.
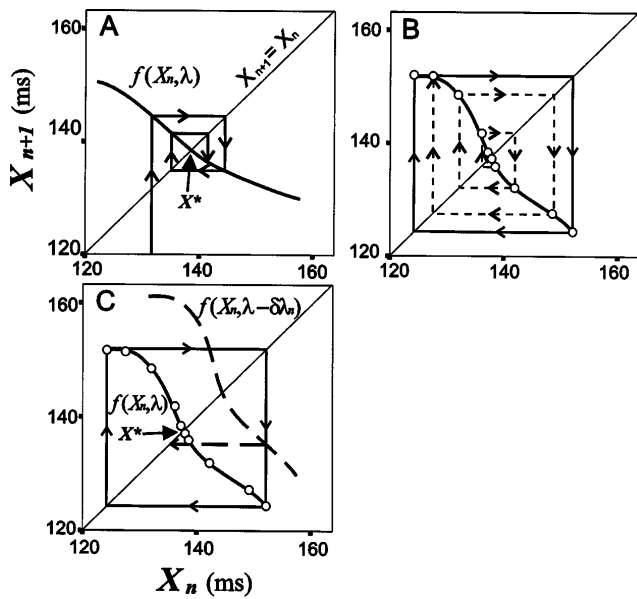

FIG. 2. The difference equation, $X_{n+1} = f(X_n, \lambda)$, relating successive AV nodal conduction times and a schematic of the control mechanism. (a) Convergence of successive conduction times to a stable fixed point, X^*, when the slope of $f(X_n, \lambda)$ at X^* is greater than -1. (b) Development of alternans in one of our preparations when the slope of $f(X_n, \lambda)$ at X^* was less than -1. (c) Effect of a premature stimulation, $\lambda - \delta\lambda_n$, on f. A premature stimulation applied after a beat with a long AV nodal conduction time directs the subsequent conduction time closer to X^* (dashed arrow).

of alternans (solid arrows) for one of our preparations. Slow nonstationary effects are associated with gradual deformations of f over several iterations, which can both shift X^* and change the slope of f at X^*.

Since alternans arise when a fixed point loses stability in the manner described above, the unstable fixed point must lie between the alternating X's. Control of alternans can be achieved by directing the system towards the unstable fixed point by varying λ for certain beats [7]. This procedure is schematically depicted in Fig. 2(c). By shortening λ by an appropriate amount $\delta\lambda_n$ after a large X_n, the map f shifts to the dashed curve. The subsequent X_{n+1} is thereby directed closer to the unstable fixed point X^* as shown by the dashed arrow.

The simplest way to choose the magnitude of $\delta\lambda_n$ is to make it proportional to the distance between the system's present state point, X_n, and the unstable fixed point. Therefore, the stimulus delay time for beat $n + 1$ was shortened by an amount $\delta\lambda_n$, where

$$\delta\lambda_n = \alpha(X_n - \hat{X}^*).$$

The proportionality constant α established the sensitivity of the control algorithm. $\hat{X}^*$ was the current estimate of X^* approximated as the midpoint of the alternating X's

$$\hat{X}^* = \frac{1}{2}(X_n + X_{n-1}).$$

This fixed point estimate was recomputed after each beat allowing us to adaptively locate the real fixed point. It is not necessary to know the analytic form of f to apply this algorithm.

We used this control method to suppress alternans rhythms in five rabbit heart preparations in which AV nodal conduction was impaired [12]. The left panels of Fig. 3 show the sequence of AV nodal conduction times X_n before, during, and after the control period along with the corresponding values for λ_n in three different preparations. The right panels are points of f obtained during the transient periods at the onset ($+$) and following the termination ($\bullet$) of the control. Figure 3(a) shows control of nonstationary alternans which have an increasing magnitude and a slow average drift of the AV nodal conduction time. Because the unstable fixed point was adaptively lo-
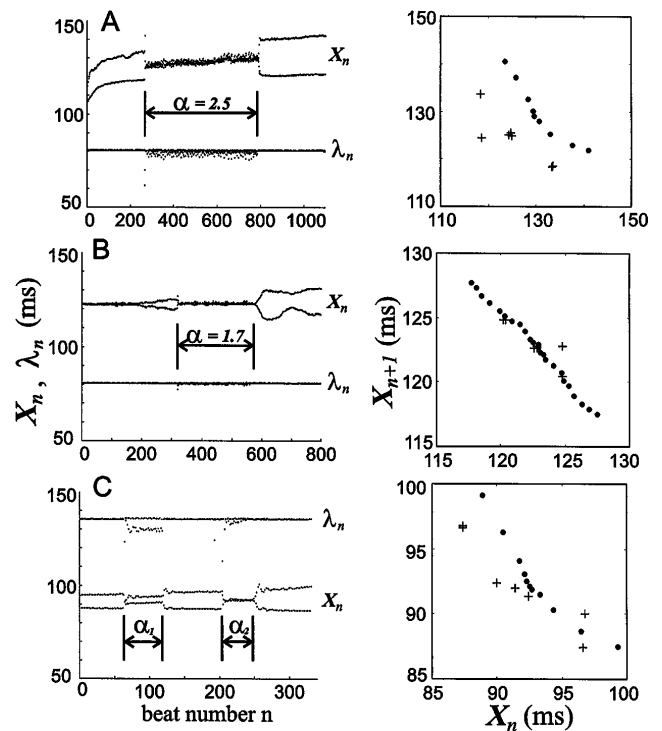

FIG. 3. Control of alternans in three preparations. (a) AV nodal conduction times X_n and delay times λ_n in the first preparation. Control was implemented from beat 266 to 787 (2 min) with $\alpha = 2.5$. The right panel plots X_{n+1} versus X_n at the onset ($+$) and following the termination ($\bullet$) of the control sequence. The fixed point X^* after the control was 130 ms and the slope of the map at this point was -1.7. (b) X_n and λ_n in the second preparation. Control was implemented from beat 319 to 550 for $\alpha = 1.7$. X^* after the control was 123 ms and the slope at the fixed point was -1.2. (c) X_n and λ_n in the third preparation. The first control attempt was implemented from beat 79 to 134 with $\alpha_1 = 3.3$. The second control attempt was implemented from beat 219 to 255 with $\alpha_2 = 5.0$. After the second control, X^* was 92 ms and the slope at the fixed point was -1.5.

cated, its evolution was tracked. The right panel shows the shift of f over the course of the control. Figure 3(b) shows that when control was initiated near the onset of alternans, relatively small perturbations (less than 2 ms) were required to suppress its development. In this case, the unstable fixed point did not evolve appreciably over the course of the control.

The control technique requires that we choose an appropriate proportionality constant α. In our experiments, α was chosen by trial and error. If α was too small the alternans magnitude was reduced, but not eliminated. For example, the preparation depicted in Fig. 3(c) shows that the first control attempt, with $\alpha_1 = 3.3$, was not sufficient to eliminate the alternans. The next attempt, with $\alpha_2 = 5.0$, was successful. These observations led us to examine the stability conditions of the controlled system.

Turning on the control algorithm had the effect of transforming the one-dimensional map (1) into the following two-dimensional system:

$$X_{n+1} = f\left(X_n, \lambda - \frac{\alpha}{2}(X_n - Y_n)\right)$$
$$Y_{n+1} = X_n \tag{2}$$

The period-1 fixed point of this system (X^*, Y^*) has the property $X^* = Y^*$, which is also the value of the uncontrolled system's fixed point. The Jacobian of this system is

$$\begin{bmatrix} A - \frac{\alpha}{2}B & \frac{\alpha}{2}B \\ 1 & 0 \end{bmatrix}, \tag{3}$$

where $A = \frac{\partial f}{\partial X}$ and $B = \frac{\partial f}{\partial \lambda}$. In our case, both A and B are negative at the fixed point.

The fixed point is stable provided that the Jacobian has eigenvalues which fall within the unit circle. This condition is met for α in the following range:

$$\frac{(|A| - 1)}{|B|} < \alpha < \frac{2}{|B|},$$

where all terms are evaluated at the fixed point. Although it is not necessary to know the analytic form of f to apply the control algorithm, the properties of the map determine the range of α which gives effective control.

Because many beats had conduction times which were less than $\hat{X}^*$, $\delta\lambda_n$ was often negative, implying that the stimulus should have been delayed for those beats. However, in clinical situations where alternans occur naturally, beats induced via electrical stimulation can only shorten λ. Therefore, premature stimuli were delivered only after beats with conduction times larger than $\hat{X}^*$. Otherwise, $\delta\lambda_n$ was set to zero and the stimulus was delivered at the unperturbed delay, λ. This modification doubles the lower limit of effective α and the upper limit increases by a presently unknown amount.

To estimate the lower limits of effective α in our experiments, we assumed that f had the following form:

$f(X_n, \lambda) = a + \exp(-\lambda/\tau)h(X_n)$, where a and τ are parameters which can be determined experimentally, and h is an unknown decreasing function [11]. Therefore, at the fixed point $B = -\frac{1}{\tau}(X^* - a)$. Previous studies have shown that typical values for a and τ are 80 and 70 ms, respectively [11]. Using these parameters, and X^* and A determined from the maps in Fig. 3, we estimated that the lower limits of effective α are 2, 0.7, and 5 for the preparations shown in Figs. 3(a), 3(b), and 3(c), respectively. These limits agree with our observations.

In some preparations the alternans rhythm was more complex. For example, Fig. 4(a) shows irregular oscillations superimposed over each alternans branch. This kind of behavior is seen when the curve f shifts back and forth with a period of about 20 beats (not shown). The physiological mechanism of such a nonstationarity is unknown. Nevertheless, the control algorithm successfully eliminated these irregular alternans [Figs. 4(b) and 4(c)], thus showing that the technique is robust to complex rhythms.

Previous biological control experiments implemented a precontrol learning phase to estimate X^* which was held constant over the course of the control [5]. Any error in the fixed point estimate leads to a controlled fixed point which differs from that of the uncontrolled system. Furthermore, an evolving fixed point of the original system cannot be tracked using such a scheme.

Since we recomputed our fixed point estimate $\hat{X}^*$ after each beat, our control algorithm accurately targeted the
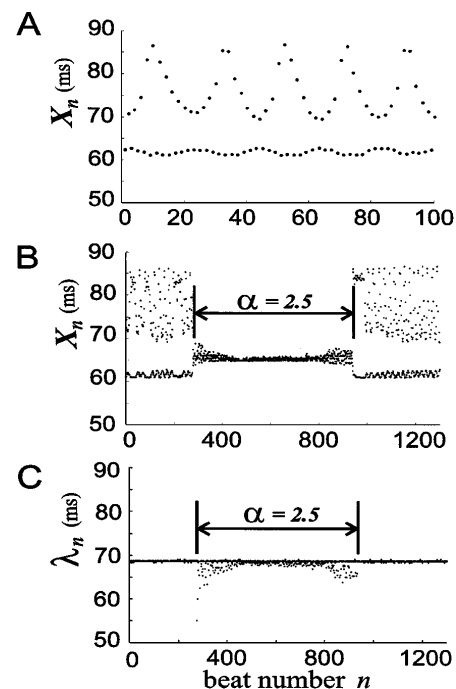

FIG. 4. Control of complex alternans. (a) 100 beats of X_n showing an irregular oscillation superimposed over each alternans branch. (b) X_n with control implemented from beat 277 to beat 936 with $\alpha = 2.5$. (c) Corresponding λ_n.

original system's unstable period-1 fixed point. Slow evolution of the fixed point was tracked. However, since f slowly evolves, the limits on the range of effective α correspondingly change. Therefore, while α may initially be in the effective range, the system's evolution may lead to destabilization. In most cases, the range of effective α was sufficiently large so that the gradual evolution of the system did not destabilize the fixed point.

Suppression of cardiac alternans has important clinical implications given that alternans in the electrocardiogram morphology often precedes life-threatening arrhythmias and is a risk factor for sudden death [8]. If a control algorithm similar to the one used in the present study was incorporated in a prosthetic cardiac pacemaker, such alternans rhythms might be suppressed and a route to a fatal arrhythmia curtailed.

---

[1] E. Ott, C. Grebogi, and J.A. Yorke, Phys. Rev. Lett. **64**, 1196–1199 (1990).

[2] W.L. Ditto, S.N. Rauseo, and M.L. Spano, Phys. Rev. Lett. **65**, 3211 (1990); E.R. Hunt, Phys. Rev. Lett. **67**, 1953 (1991); B. Peng, V. Petrov, and K. Showalter, J. Phys. Chem. **95**, 4957 (1991); V. Petrov, B. Peng, and K. Showalter, J. Chem. Phys. **96**, 7505–7513 (1992); R. Roy, T.W. Murphy, T.D. Maier, Z. Gills, and E.R. Hunt, Phys. Rev. Lett. **68**, 1259 (1992).

[3] T.L. Carroll, I. Triandaf, I.B. Schwartz, and L. Pecora, Phys. Rev. A **46**, 6189 (1992); Z. Gills, C. Iwata, R. Roy, I.B. Schwartz, and I. Triandaf, Phys. Rev. Lett. **69**, 3169 (1992); I.B. Schwartz and I. Triandaf, Phys. Rev. A **48**, 718 (1993); V. Petrov, M.J. Crowley, and K. Showalter, Phys. Rev. Lett. **72**, 2955 (1994); N.F. Rulkov, L.S. Tsimring, and H.D.I. Abarbanel, Phys. Rev. E **50**, 314 (1994).

[4] M.E. Josephson, *Clinical Cardiac Electrophysiology: Techniques and Interpretation* (Lea Febiger, Philadelphia, 1993), 2nd ed.; *From Cell to Bedside: Cardiac Electrophysiology,* edited by D. Zipes and J. Jalife (W.B. Saunders, Philadelphia, 1995).

[5] A. Garfinkel, M.L. Spano, W.L. Ditto, and J.N. Weiss, Science **257**, 1230–1235 (1992); S.J. Schiff, K. Jerger, D.H. Duong, T. Chang, M.L. Spano, and W.L. Ditto, Nature (London) **370**, 615–620 (1994).

[6] L. Glass and W. Zeng, Int. J. Bifurcation Chaos **4**, 1061–1067 (1994); D.J. Christini and J.J. Collins, Phys. Rev.

[7] Lett. **75**, 2782–2785 (1995); T.L. Carroll, Phys. Rev. E **52**, 5817 (1995); M.E. Brandt and G. Chen, Biol. Cybern. **74**, 1–8 (1996); M.E. Brandt and G. Chen, Int. J. Bifurcation Chaos **6**, 715–723 (1996).

[7] D.J. Christini and J.J. Collins, Phys. Rev. E **53**, R49–R52 (1996). Our control algorithm is a modified version of the one used in this modeling study. Our modifications ensured that the algorithm changed the stability, but not the location, of the uncontrolled system's unstable period-1 fixed point.

[8] J.M. Smith, E.A. Clancy, C.R. Valeri, J.N. Ruskin, and R.J. Cohen, Circulation **77**, 110–121 (1988); D.S. Rosenbaum, L.E. Jackson, J.M. Smith, H. Garan, J.N. Ruskin, and R.J. Cohen, N. Eng. J. Med. **330**, 235–241 (1994).

[9] T. Lewis, Q. J. Med. **4**, 141 (1910–1911); T. Lewis and G.C. Mathison, Heart **2**, 47–53 (1910).

[10] The right atrium, AV nodal area, and upper part of the ventricular septum were dissected and mounted in a tissue bath perfused at 200 mℓ/min with a 6-ℓ volume of oxygenated (95% O_2, 5% CO_2) Tyrode solution maintained at 37 °C and pH 7.38. Its composition (in mM) was 128.2 NaCl, 4.7 KCl, 2.0 $CaCl_2$, 1.0 $MgCl_2$, 20.0 $NaHCO_3$, 0.7 NaH_2PO_4, and 11.1 dextrose. Four unipolar silver recording electrodes were placed on the surface of the preparation: one at the upper atrium, two at the AV nodal inputs (i.e., the low crista terminalis and the low interatrial septum), and one at the His bundle. A bipolar platinum-iridium stimulation electrode was placed on the upper atrium near the sinus node. Voltage pulses of 2 ms in duration and 1.2 V in amplitude were used to pace the tissue such that the time interval, λ, between His bundle activation and the delivery of the next atrial stimulus was fixed for each pacing rate. Activation times, defined by the negative peaks of the first time derivatives of the electrograms, were determined with 0.25 ms precision. Time intervals between the activations of the three atrial recording sites, the His bundle, and the stimulation pulses were determined with 0.35 ms precision. The AV nodal conduction time, X, was defined as the time interval between the activations of the low interatrial septum and His bundle.

[11] J. Sun, F. Amellal, L. Glass, and J. Billette, J. Theor. Biol. **173**, 79 (1995); F. Amellal, K. Hall, L. Glass, and J. Billette, J. Cardiovasc. Electrophysiol. **7**(10), 943–951 (1996).

[12] The alternans magnitude increased when the electrical excitability of the preparation was decreased by either inducing transient hypoxia ($n = 2$), or using a combination of hypoxia and the calcium channel blocker verapamil (30 ng/mℓ) ($n = 3$).